Using Drifter Velocity Measurements to Assess and Constrain Coarse-Resolution Ocean Models

MENGNAN ZHAO,[a] RUI M. PONTE,[a] OU WANG,[b] AND RICK LUMPKIN[c]

[a] *Atmospheric and Environmental Research, Inc., Lexington, Massachusetts*
[b] *Jet Propulsion Laboratory, California Institute of Technology, Pasadena, California*
[c] *Physical Oceanography Division, NOAA/Atlantic Oceanographic and Meteorological Laboratory, Miami, Florida*

(Manuscript received 5 October 2020, in final form 2 February 2021)

ABSTRACT: Properly fitting ocean models to observations is crucial for improving model performance and understanding ocean dynamics. Near-surface velocity measurements from the Global Drifter Program (GDP) contain valuable information about upper-ocean circulation and air–sea fluxes on various space and time scales. This study explores whether GDP measurements can be used for usefully constraining the surface circulation from coarse-resolution ocean models, using global solutions produced by the consortium for Estimating the Circulation and Climate of the Ocean (ECCO) as an example. To address this problem, a careful examination of velocity data errors is required. Comparisons between an ECCO model simulation, performed without any data constraints, and GDP and Ocean Surface Current Analyses Real-Time (OSCAR) velocity data, over the period 1992–2017, reveal considerable differences in magnitude and pattern. These comparisons are used to estimate GDP data errors in the context of the time-mean and time-variable surface circulations. Both instrumental errors and errors associated with limitations in model physics and resolution (representation errors) are considered. Given the estimated model–data differences, errors, and signal-to-noise ratios, our results indicate that constraining ocean-state estimates to GDP can have a substantial impact on the ECCO large-scale time-mean surface circulation over extensive areas. Impact of GDP data constraints on the ECCO time-variable circulation would be weaker and mainly limited to low latitudes. Representation errors contribute substantially to degrading the data impacts.

KEYWORDS: Ocean circulation; Error analysis; Climate models; Data assimilation

1. Introduction

Knowledge of ocean surface currents is essential for diverse applications, such as tracing the origins and the fate of physical/biogeochemical particles (e.g., Pringle et al. 2014; Aleynik et al. 2016), studying ocean energetics and instabilities (e.g., Elipot and Gille 2009; Lumpkin and Flament 2013), examining waves and tides (e.g., Kawaguchi et al. 2015; Hui and Xu 2016; Lozovatsky et al. 2016), and inferring velocity fields at depth (e.g., Wunsch 1997; de La Lama et al. 2016). Surface drifters, deployed since 1979 as part of the Global Drifter Program (GDP; formally referred to as the Surface Velocity Program), directly measure the velocity field at a nominal depth of ~15 m. Despite uneven temporal and spatial distributions, drifter velocity data are able to capture all dynamic components, unlike estimates based on satellite altimetry, which provide only geostrophic velocity and require an accurate depiction of the ocean mean dynamic topography (MDT) (e.g., Rio et al. 2014), and wind-derived Ekman velocities that additionally depend on uncertain parameters in basic Ekman layer theory (e.g., Sudre et al. 2013).

Many previous studies have taken advantage of the high temporal (~hourly) and spatial (~a few kilometers) resolution of the drifter velocity data for model validation (e.g., Johnson et al. 2007; Blockley et al. 2012), understanding small-scale processes such as turbulent flows and lateral diffusion (e.g., Sallée et al. 2008; Qian et al. 2014) and the assessment of high-resolution model performance (e.g., Yu et al. 2019). Such analyses can be used to improve subgrid-scale parameterizations in ocean models. For example, Zhurbas and Oh (2003) presented a parameterization of mixing for the midlatitude Pacific Ocean calibrated using drifter-derived lateral diffusivity estimates. Using drifter measurements to examine model simulations of the large-scale surface circulation on climate time scales has not been explored as much (e.g., Petersen et al. 2019). In fact, relatively little is known about the realism of the variable surface circulation in relatively coarse resolution climate models, even though such currents are important for surface heat and freshwater transports and related air–sea interactions (e.g., Kelly and Dong 2004; Small et al. 2008; Drews and Greatbatch 2016; Müller et al. 2019).

Drifter data have been combined with gravity, sea level, density, and other data to derive MDT fields (e.g., Kubryakov and Stanichny 2011; Knudsen et al. 2021), but such practice involves removing estimates of the ageostrophic flows contained in the drifter observations. One way to use all the information in the drifter velocity data is through data assimilation methods (e.g., Wunsch et al. 2009; Sun and Penny 2019) that formally constrain models to observations. The consortium for Estimating the Circulation and Climate of the Ocean (ECCO), an example of such an effort, has been providing global ocean-state estimates by constraining a general circulation model to most available ocean observations in a weighted least squares sense (e.g., Wunsch et al. 2009; Forget et al. 2015). The ECCO solutions are optimized via a process using the method of Lagrange multipliers (e.g., Forget et al. 2015), by which atmospheric boundary conditions, internal model parameters and initial conditions are adjusted to minimize the overall model–data misfits to within expected uncertainties. Despite many model constraints from temperature, salinity, bottom pressure, sea level and MDT data, ECCO velocity fields

Corresponding author: Mengnan Zhao, mzhao@aer.com

DOI: 10.1175/JTECH-D-20-0159.1

© 2021 American Meteorological Society. For information regarding reuse of this content and general copyright information, consult the AMS Copyright Policy (www.ametsoc.org/PUBSReuseLicenses).

Brought to you by NOAA Central Library | Unauthenticated | Downloaded 04/20/21 02:47 PM UTC

have not been constrained by direct velocity measurements. Assimilation of surface drifter currents in other similar efforts is unknown to us. A basic question thus is whether GDP measurements could be important in improving the surface circulation in climate analyses such as those produced by ECCO, on monthly or longer (climatological) time scales.

To begin addressing such question, we take advantage of the ECCO framework and use an available model experiment, performed without any data constraints, to assess the simulated surface currents against the GDP observations. The calculated model–data differences provide a basic description of possible deficiencies in the simulated surface velocities. In addition, the model and GDP differences can be used to derive data errors. Constraining models to data requires a careful examination of such errors, including both instrument errors and representation errors. Regarding instrument errors, besides data noise, the GDP drifter measurements are also subject to uncertainties in the drifters' position fixes, wind, and wave-driven slip biases. The representation errors arise from signals that can be detected by the measurements but are not represented in the model due, for example, to lack of sufficient resolution or relevant physics. For instance, the coarse resolution in ECCO version 4 does not allow for the representation of mesoscale processes contained in GDP measurements, leading to significantly reduced eddy kinetic energy near strong current systems. (We will use "data errors" throughout to mean the combined instrument and representation errors.) Proper estimation of data errors helps avoid underfitting or overfitting of models to observations: underfitting happens when unrealistically large errors lead to an insufficient use of the information in the data; overfitting involves underestimated data errors that can lead to fitting unwanted data noise. The data errors inferred from model and data comparisons carried out here are then used to evaluate the model–data misfits on daily, monthly, and climatological time scales and shed light on whether constraining to GDP observations can potentially lead to a better representation of the surface circulation in climate models.

The paper is structured as follows. Section 2 provides details of the drifter data and ECCO output, as well as the Ocean Surface Current Analyses Real-Time (OSCAR) velocity product also used in the study. Methods to estimate GDP data errors are also presented. In section 3, time-variable and time-mean velocity fields and basic statistics of misfits between ECCO model simulations and GDP measurements are examined. Section 4 describes data errors on daily, monthly, and climatological time scales and discusses, in the context of ECCO, the feasibility of constraining climate model analyses with the global drifter currents.[1] A summary and discussion of our findings are presented in section 5.

[1] In this study, we use the Eulerian instead of Lagrangian approach to understand the potential of using GDP data to constrain ECCO surface currents. The Eulerian method is easier to explore given that horizontal velocities are a prognostic variable of ECCO and most other modeling frameworks, and simple estimates of uncertainty are also feasible. The use of the Lagrangian approach is beyond the scope of our current study and may be pursued in the future.

2. Velocity products and methods

a. *ECCO, GDP, and OSCAR velocities*

1) ECCO FIELDS

ECCO provides global ocean-state estimates by constraining the Massachusetts Institute of Technology general circulation model (MITgcm) to observational data in a physically and statistically consistent manner (https://www.ecco-group.org/). For different research purposes, several versions of ECCO products have been released with various resolutions, temporal coverage, physics, observational data, and assimilation methods. In this study, we use an ECCO version 4 release 4 control run, which is an initial run of the ocean model without any data constraints. (Such runs serve as the starting point for the iterative optimization procedure that brings the model closer to available data to produce the ECCO state estimates.) Full details of the ECCO version 4 release 4 (and previous releases) model setup used here are provided in Forget et al. (2015) and Fukumori et al. (2017, 2019). The model is run on a global grid with forcing from surface atmospheric variables from the European Centre for Medium-Range Weather Forecasts interim reanalysis (ERA-Interim; Dee et al. 2011), including surface pressure fields as described in Fukumori et al. (2019). Initial conditions are those used to start the optimization for ECCO version 4 release 4 (Fukumori et al. 2019). The horizontal resolution varies from 22 to 111 km: highest in high latitudes and lowest in midlatitudes (Wang et al. 2019). Daily zonal and meridional velocities are available globally from 1 January 1992 to 30 December 2017 on the model native grids over 50 vertical levels. Velocities at the second vertical level (nominally 15 m), which represent mean values over 10–20 m depth, are used to compare with drifter measurements.

2) GDP DATA

The GDP (https://www.aoml.noaa.gov/phod/gdp/; Lumpkin and Centurioni 2019) offers direct measurements of mixed layer currents. Each drifter consists of a surface float with an antenna that reports drifter locations to satellites. A drogue at 15 m is attached to the surface float, to minimize the surface float sliding caused by winds or waves. Pseudo-Eulerian surface horizontal velocities are derived from the drifter positions. First deployed in 1979, drifters cover almost 80% of the global ocean in 5° × 5° bins and thus provide a valuable dataset to examine ocean surface currents on very short (hourly) to longer (climatological) scales.

Raw data are processed at NOAA's Atlantic Oceanographic and Meteorological Laboratory (AOML). After interpolation via kriging to 6 h intervals (Hansen and Poulain 1996), these velocity data are corrected for the "slip" effects induced by winds and waves by removing a fraction of downwind velocity component following Niiler et al. (1995). The slip correction is applied to both drogued and drogue-lost drifters. Considering that drogue-lost drifters are more susceptible to winds, higher fractions of downwind velocities are removed in slip correction for drogue-lost than for drogued drifters (Poulain et al. 2009; Laurindo et al. 2017). The corrected velocities from undrogued drifters have been found to be reliable and consistent with

Brought to you by NOAA Central Library | Unauthenticated | Downloaded 04/20/21 02:47 PM UTC

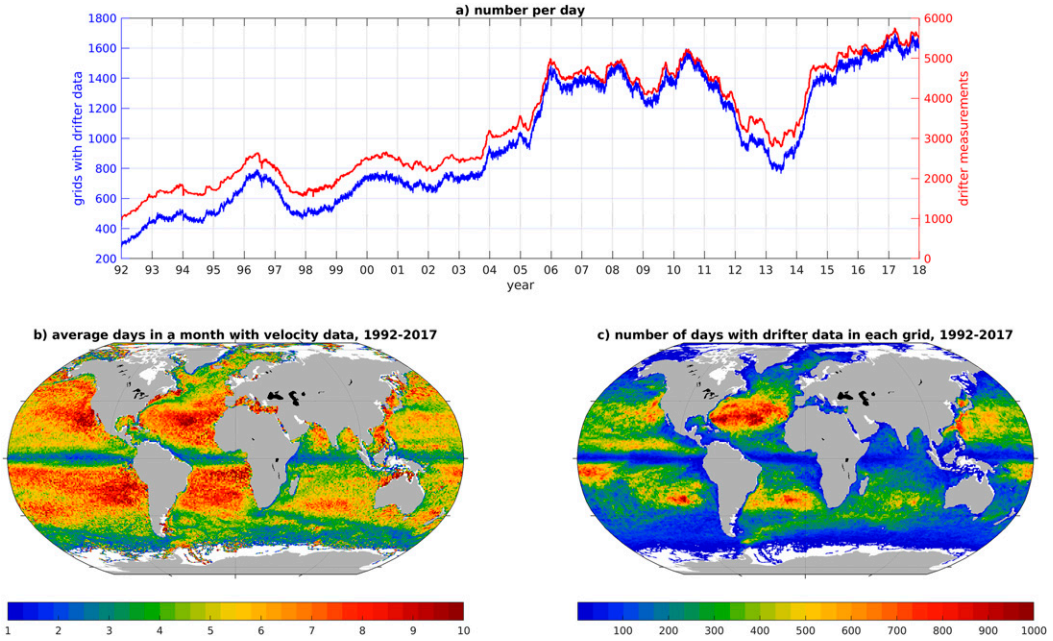

FIG. 1. (a) Number of grids with drifter data per day (blue) and total drifter measurements per day (red) from 1992 to 2017. (b) Average number of days with drifter data per month over 1992–2017. (c) Total number of days with drifter data over 1992–2017.

those from drogued drifters (Laurindo et al. 2017). Therefore, we use velocities from both kinds to maximize the data quantity. A low-pass filter is then applied to the original processing at AOML with a cutoff period of 1.5 times the local inertial period, with a minimum of 1 day and a maximum of 5 days. The filter removes high frequency signals such as tides and inertial motions. Velocity data used in this study refer to the period between 1979 and 2017.

3) OSCAR PRODUCT

The OSCAR product is a global surface mixed layer current database [https://www.esr.org/research/oscar/; Earth and Space Research (ESR); ESR 2009; Bonjean and Lagerloef 2002], representing the average velocity of the upper 30 m of the water column. The estimates are calculated using a quasi-steady geostrophic model together with a wind-driven ageostrophic component and a thermal wind adjustment, derived from sea surface height, wind stress and sea surface temperature data (Hausman et al. 2009). Near the equator where geostrophy breaks down (the Coriolis parameter approaches zero), the model is adjusted so that the pressure gradient force and the wind drag force terms are balanced to zero order (Bonjean and Lagerloef 2002). The resultant velocities have been validated with equatorial ADCP currents (Johnson et al. 2007). Temporal coverage is from October 1992 to present at intervals of 5 days on 1/3° × 1/3° grids. Each value at a given time is derived from satellite data within a 10-day window; i.e., velocities at adjacent time intervals are not fully independent. We use OSCAR velocities to compare with the ECCO and GDP fields and also to estimate the drifter data errors on climatological time scales.

b. *Calculation of daily, monthly, and climatological velocity field*

For the purpose of this study, the 6-hourly drifter velocity data are first mapped onto the ECCO grid to create daily drifter velocity field. All GDP velocities on a given day within each ECCO grid cell are first selected and then averaged to provide a daily velocity on each cell. Note that there are many days when no drifter measurements are available on any given grid cell. Drifter measurements are unevenly distributed both temporally and spatially (Fig. 1). A higher concentration of drifter data is found in the Ekman convergence zones (i.e., interior of subtropical basins; Figs. 1b,c). The number of drifter measurements increases from 1992 to 2017 (Fig. 1a).

Daily ECCO model velocities used in this study are those with spatial and temporal coverage corresponding to where and when interpolated daily drifter velocities are available. Monthly ECCO and drifter velocity fields are calculated as the temporal mean of daily velocities (when available) over each month. Due to the uneven GDP data distribution, only a few daily fields are usually available to estimate any monthly value (Fig. 1b).

In addition to daily and monthly fields, a velocity climatology is estimated from daily fields for each of the three products in section 2a. We first spatially average OSCAR velocities at each time onto the ECCO grid as done with GDP data. To account for the coarser temporal resolution of OSCAR data, on each grid, mean values of GDP and ECCO velocities over 10 days centered on OSCAR time steps are computed. The OSCAR data are not used when no GDP data are available. To this end, the three products are processed to the same temporal

Brought to you by NOAA Central Library | Unauthenticated | Downloaded 04/20/21 02:47 PM UTC

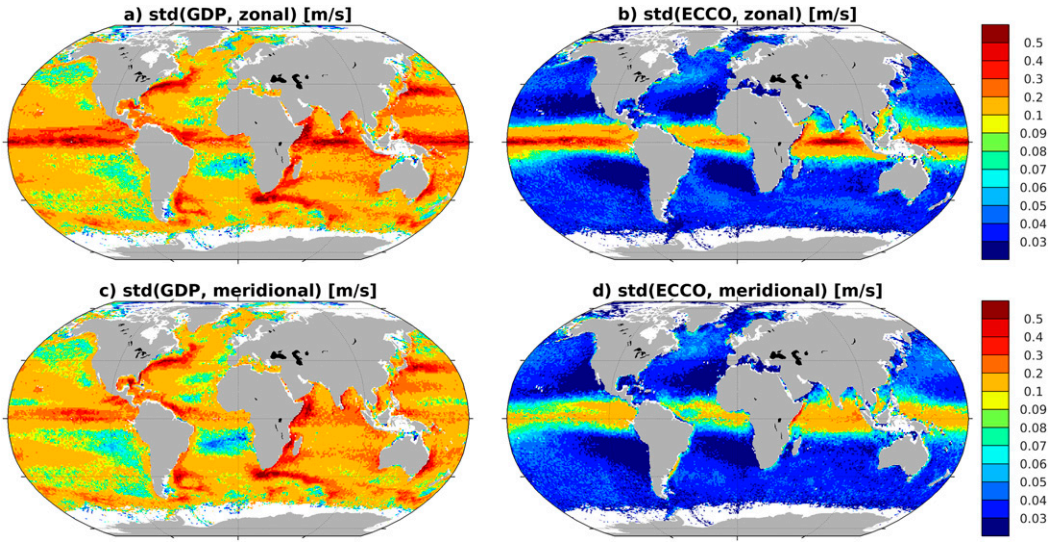

FIG. 2. (top) Standard deviation of daily zonal velocities from (a) GDP and (b) ECCO. (bottom) Standard deviation of daily meridional velocities from (c) GDP and (d) ECCO. Note the nonlinear color bar.

and spatial resolution and coverage and then time averaged to arrive at the climatological currents.

c. Calculation of errors

We introduce the methods used to estimate errors for GDP data for the purpose of discussing possibility of constraining climate models with drifter data. Again, as stated in the introduction, we seek estimates that contain both instrument and representation errors, with the latter defined in the context of the ECCO version 4 model setup used in this work. As it is useful when implementing data constraints to examine separately time-variable and time-mean misfits, we examine respective errors separately below.

The calculation of errors for time-variable GDP velocities ε_D follows Quinn and Ponte (2008) and Vinogradova et al. (2014). Denoting the "true," measured, and modeled velocity to be s, D, and M, respectively, then

$$D = s + \varepsilon_D, \tag{1}$$

$$M = s + \varepsilon_M, \tag{2}$$

where ε_D (ε_M) is the error associated with measured (modeled) velocity.

The difference between variances of Eqs. (1) and (2) yields

$$\mathrm{var}(D) - \mathrm{var}(M) = \mathrm{var}(\varepsilon_D) - \mathrm{var}(\varepsilon_M) + 2\mathrm{cov}(s, \varepsilon_D) - 2\mathrm{cov}(s, \varepsilon_M), \tag{3}$$

and the variance of Eq. (1) − Eq. (2) gives

$$\mathrm{var}(D) + \mathrm{var}(M) = 2\mathrm{cov}(D, M) + \mathrm{var}(\varepsilon_D) + \mathrm{var}(\varepsilon_M) - 2\mathrm{cov}(\varepsilon_D, \varepsilon_M), \tag{4}$$

where var and cov are the variance and covariance operators. Adding Eq. (3) to Eq. (4), we obtain an estimate of data error variances as

$$\mathrm{var}(\varepsilon_D) = \mathrm{var}(D) - \mathrm{cov}(D, M) - \mathrm{cov}(s, \varepsilon_D) + \mathrm{cov}(s, \varepsilon_M) + \mathrm{cov}(\varepsilon_D, \varepsilon_M). \tag{5}$$

Assuming the true signal s, errors ε_D and ε_M are uncorrelated, i.e., the last three terms in Eq. (5) can be neglected, data error variances can be estimated from measured and modeled velocities following

$$\mathrm{var}(\varepsilon_D) = \mathrm{var}(D) - \mathrm{cov}(D, M). \tag{6}$$

Under the assumption of uncorrelated s, ε_D and ε_M, Eq. (4) can be written as $\mathrm{var}(\varepsilon_D) + \mathrm{var}(\varepsilon_M) = \mathrm{var}(D - M)$. Therefore, the maximum value of $\mathrm{var}(\varepsilon_D)$ is $\mathrm{var}(D - M)$ when the assumption is appropriate. Since $\mathrm{var}(\varepsilon_M)$ is unlikely to be 0 and to avoid overestimating data errors, we cap $\mathrm{var}(\varepsilon_D) \leq 90\%\,\mathrm{var}(D - M)$. In addition, to mitigate unphysical (negative) estimates of errors, we bound $\mathrm{var}(\varepsilon_D) \geq 10\%\mathrm{var}(D - M)$.

We combine two complementary approaches to evaluate the errors for GDP time-mean velocity data. The first approach uses the absolute value of the difference between GDP and OSCAR climatologies (method 1 hereafter), which effectively assumes the latter to be the "truth." As the OSCAR product includes scales that are not resolved by ECCO, we use a smoothed OSCAR field obtained by averaging velocities in a 3° × 3° cell centered on a given grid point. These smoothed fields are more consistent with the spatial scales represented in the ECCO fields, and their use thus minimizes the potential underestimation of representation errors if unsmoothed OSCAR values are used instead.

A second approach uses twice the value of the standard errors of the GDP climatology discussed by Laurindo et al. (2017), provided on 1/4° × 1/4° grid (method 2 hereafter). These standard errors are associated with undersampling of mesoscale variability and limited number of samples that lead to biases in the means [see Laurindo et al. (2017) for details]. The use of twice of the standard errors follows the results of

Brought to you by NOAA Central Library | Unauthenticated | Downloaded 04/20/21 02:47 PM UTC

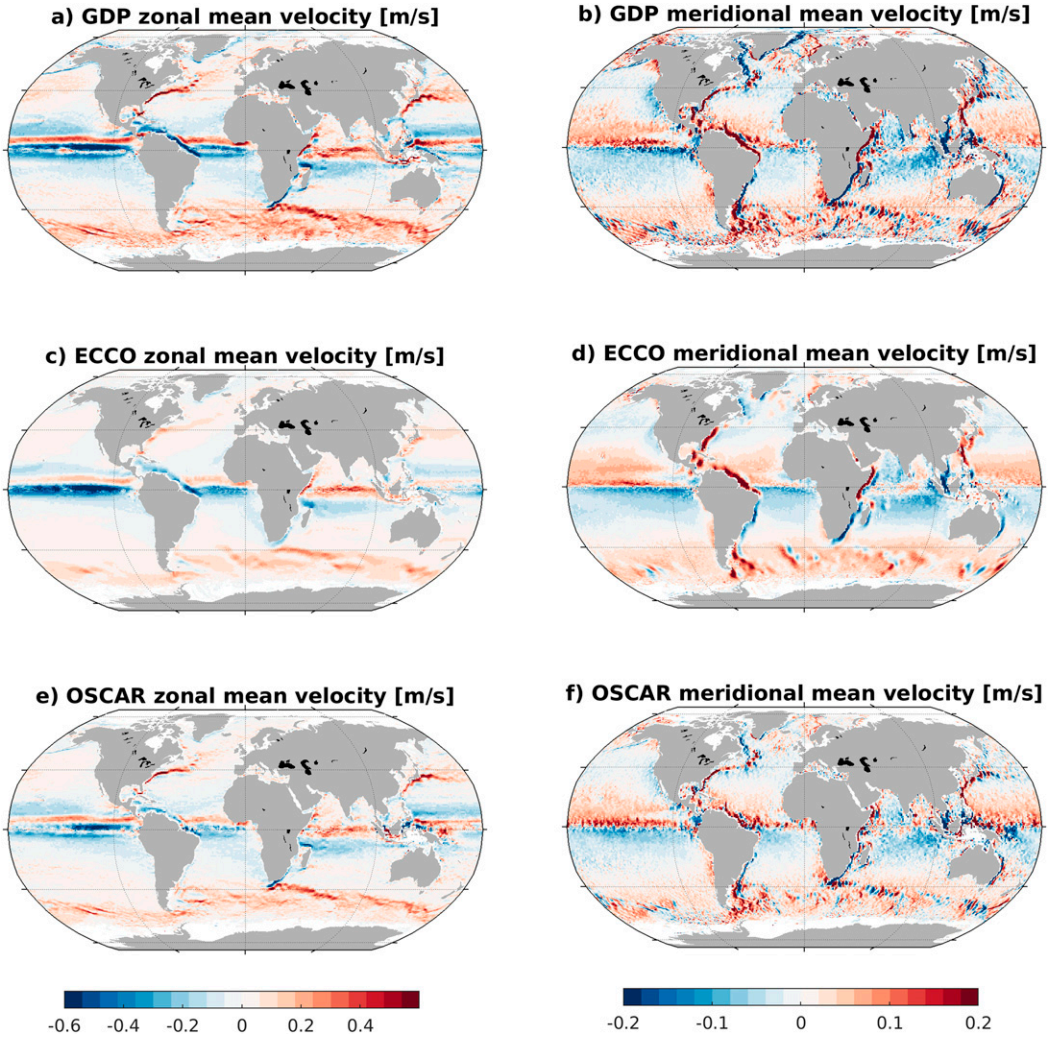

FIG. 3. (a),(c),(e) Zonal and (b),(d),(f) meridional time-mean velocity over 1992–2017 from (a),(b) GDP, (c),(d) ECCO, and (e),(f) OSCAR.

Laurindo et al. (2017) that they may be an underestimate of actual errors by a factor of 2. Errors from method 2 are then bin averaged onto the ECCO grid for further analyses.

In combining the values from the two approaches to arrive at the error fields for the climatological GDP currents, we use method 1 as the basis but limit those values to be no smaller than the errors associated with GDP sampling given by method 2. In addition, as done with errors for time-variable velocities, the square of these errors are then capped to be between 10% and 90% of the square of the ECCO and GDP differences.

d. Cost estimate

Information on data errors allows one to evaluate the potential of constraining ECCO velocity field using GDP data via properly weighted model–data misfits. In many optimization problems, the parameter used to measure whether a model M could be improved by fitting to a dataset D is the so-called cost, usually defined as $\langle (D-M)^2/\varepsilon_D^2 \rangle$, where the angle brackets $\langle\ \rangle$ denotes an average. Costs larger than one imply that the misfit between model and data exceeds the data error; therefore, optimization could be applied to the model to reduce the misfit and improve its performance.

3. Assessment of surface velocity fields

We begin by comparing the variability in GDP and ECCO control run daily velocity fields (Fig. 2). In general, standard deviations for GDP are larger than those for ECCO almost everywhere. Highest variability in GDP data occurs in regions with strong eddies associated with unstable mean currents. Variability in ECCO velocities, however, shows a different spatial pattern. Enhanced variability is located mostly near the equator and is of comparable magnitude ($\sim 0.6\,\mathrm{m\,s^{-1}}$) to that in GDP data. Regions near western boundaries and in the Southern Ocean, along the path of the Antarctic Circumpolar Current (ACC), are much quieter than what is seen in the GDP data.

The differences noted in Fig. 2 are generally consistent with expectations. More energetic GDP velocities can be mostly

Brought to you by NOAA Central Library | Unauthenticated | Downloaded 04/20/21 02:47 PM UTC

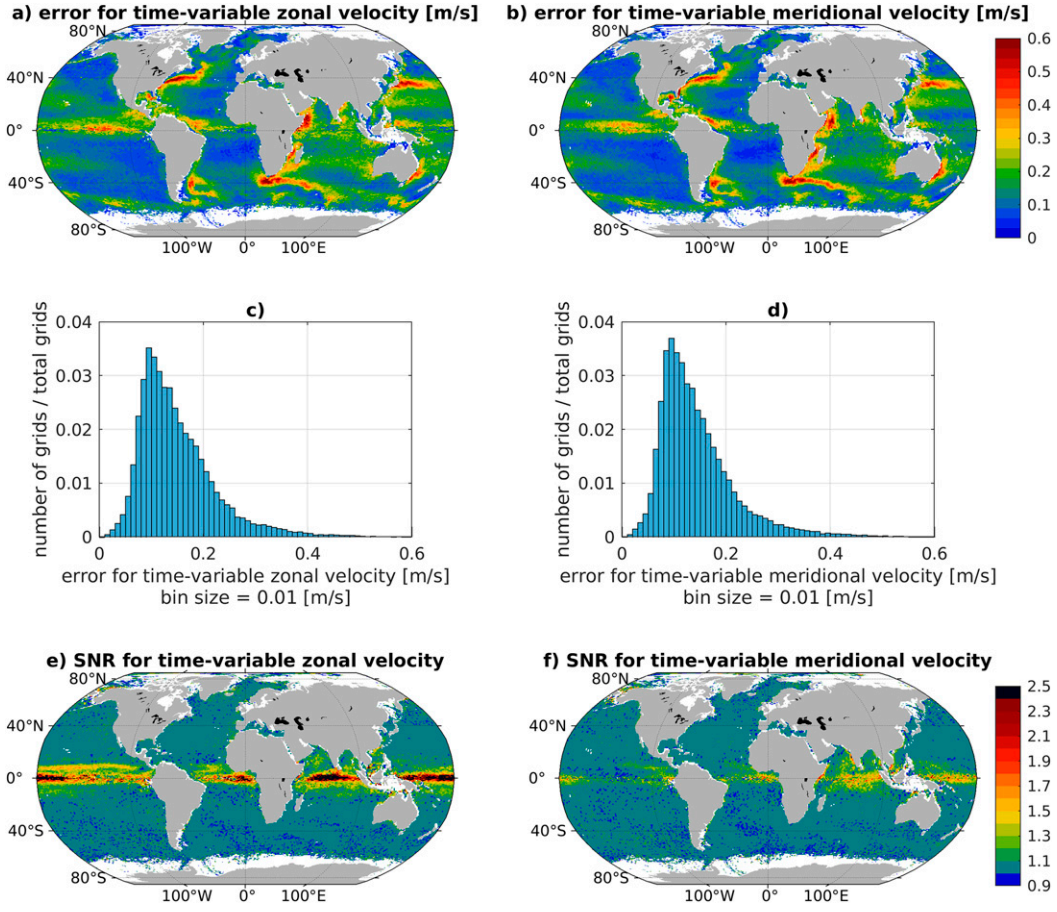

FIG. 4. (a),(b) Maps and (c),(d) histograms of errors for time-variable (daily) (a),(c) zonal and (b),(d) meridional velocities. Also shown are signal-to-noise ratios of GDP (e) zonal and (f) meridional velocities on daily time scale.

attributed to the capability of drifters to capture eddies and other smaller-scale structures, while ECCO cannot represent velocities associated with these processes due to its coarse resolution. In contrast, the closer match in magnitudes at low latitudes is consistent with the primarily wind-driven currents. Even away from western boundary regions with strong eddy activity, ECCO values are substantially weaker. Aside from the issue of resolution, it is unclear whether these discrepancies may also be related to how wind forcing, momentum transfers, and dissipation are represented in ECCO.

The standard deviations of monthly velocities (not shown) are similar to those of daily velocities in Fig. 2, both in magnitude and spatial distribution. The reason is that the monthly velocities represent the average of only a few days for which data are available, which is not sufficient to substantially suppress the submonthly variability.

The time-mean currents from GDP, ECCO and OSCAR (Fig. 3), computed using the available daily fields over 1992–2017, show reasonable agreement in their large-scale spatial patterns. Prominent currents near western boundary and equatorial regions and the ACC are all well captured in the three products. Major Ekman convergence/divergence zones, indicated by the large-scale patterns of meridional currents in opposite directions, are also compatible. Despite similar spatial patterns, the magnitude of mean currents exhibits notable differences among the three products. In particular, strong western boundary currents and their extensions as well as the ACC are visibly weaker in ECCO compared to GDP and OSCAR. The tendency for weaker circulation in ECCO is most evident for zonal currents, even in the basin interiors away from strong boundary currents. The magnitude of ECCO meridional currents are more comparable to those of GDP and OSCAR. Regarding the GDP and OSCAR climatologies, they are very comparable in pattern and magnitude, consistent with previous validation studies of OSCAR velocities using GDP (e.g., Johnson et al. 2007; Sikhakolli et al. 2013) done over different time periods.

With a lower spatial resolution, the ECCO climatology appears necessarily much smoother and weaker. In fact, an experimental, higher resolution ECCO product (version 5; https://ecco.jpl.nasa.gov/drive/files/Version5/Alpha) generates finer and stronger currents; smaller-scale features like meanders also become visible where strong eddy activity is observed. However, mean currents from drifters are also uncertain—standard errors (calculated as $\sqrt{\mathrm{var}(D)/N}$, where N indicates the number of sampling days) can be substantial compared to noted

Brought to you by NOAA Central Library | Unauthenticated | Downloaded 04/20/21 02:47 PM UTC

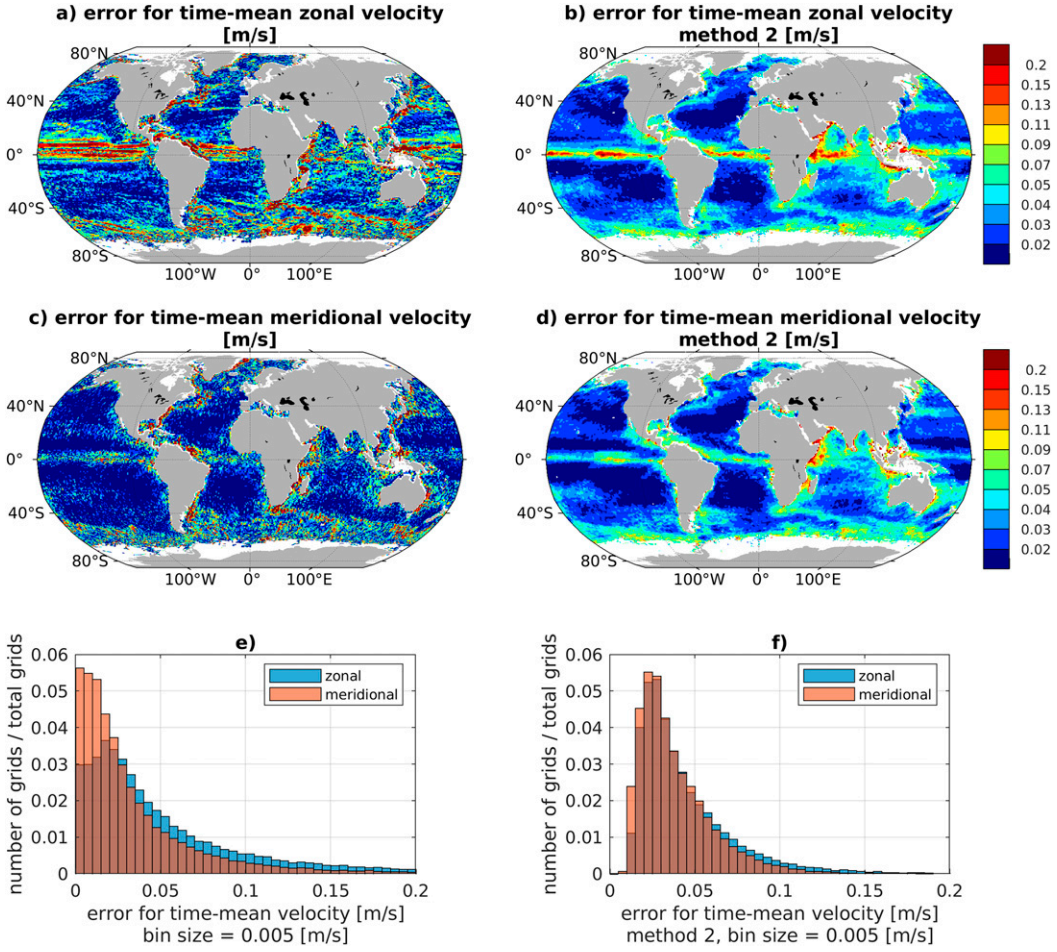

FIG. 5. (a),(c) Maps of errors for time-mean (a) zonal and (c) meridional velocities. Values are based on method 1 but first limited to be no smaller than those given by method 2, and then the square of errors are capped between 10% and 90% of the square of the ECCO and GDP differences (see section 2c). (b),(d) Maps of errors for time-mean (b) zonal and (d) meridional velocities from method 2 (see section 2c). (e)–(f) Histograms of errors in (a)–(d).

differences in ECCO and GDP velocities, particularly in the basin interiors where mean currents are also weakest. Insufficient suppression of eddy noise can be an issue: e.g., averaging velocities over all OSCAR time samplings instead of just over selected days indeed leads to weaker mean currents (not shown).

4. Assessing errors and possible GDP data constraints

a. GDP velocity errors

The majority of time-variable GDP data errors (based on daily fields) lie between 0.05 and 0.25 m s^{-1}, with the mode of the distributions ~0.1 m s^{-1} and extreme values as large as 0.6 m s^{-1} (Figs. 4a–d). Regions with large errors coincide with those of higher variability (Figs. 4a,b and 2a,c). Large uncertainties in these regions are associated with both instrument and representation errors. The instrument errors possibly stem from sampling errors (lower sampling density in these regions) and the caveats in wave-induced slip removal (Laurindo et al. 2017). The capability of drifter measurements to sample velocities at spatial scales that ECCO does not resolve can be a major source of representation errors.

The spatial distribution of our estimate of time-variable errors is comparable with that of the errors estimated by Laurindo et al. (2017), which are derived by comparing the drifter measured velocities to geostrophic velocities for mean, seasonal and residual components. However, our estimate is larger by ~0.04–0.45 m s^{-1} from basin interiors to energetic regions. Although the values from Laurindo et al. (2017) cannot exclude all representation errors, they may roughly serve as an upper limit of instrument errors. From comparing with our estimates, this indicates as expected largest representation errors in the eddy-active areas and smaller representation errors in less-energetic basin interiors. As with standard deviations, errors based on monthly fields are comparable to those based on daily fields and are not shown here.

To assess the relative relevance of the variability in GDP velocities, we examine the signal-to-noise ratio (SNR) calculated as $\sqrt{\mathrm{var}(D)/\mathrm{var}(\varepsilon_D)}$ (Figs. 4e,f). The SNR values are largest near the equator, up to 1.3–2.5, meaning that measured

Brought to you by NOAA Central Library | Unauthenticated | Downloaded 04/20/21 02:47 PM UTC

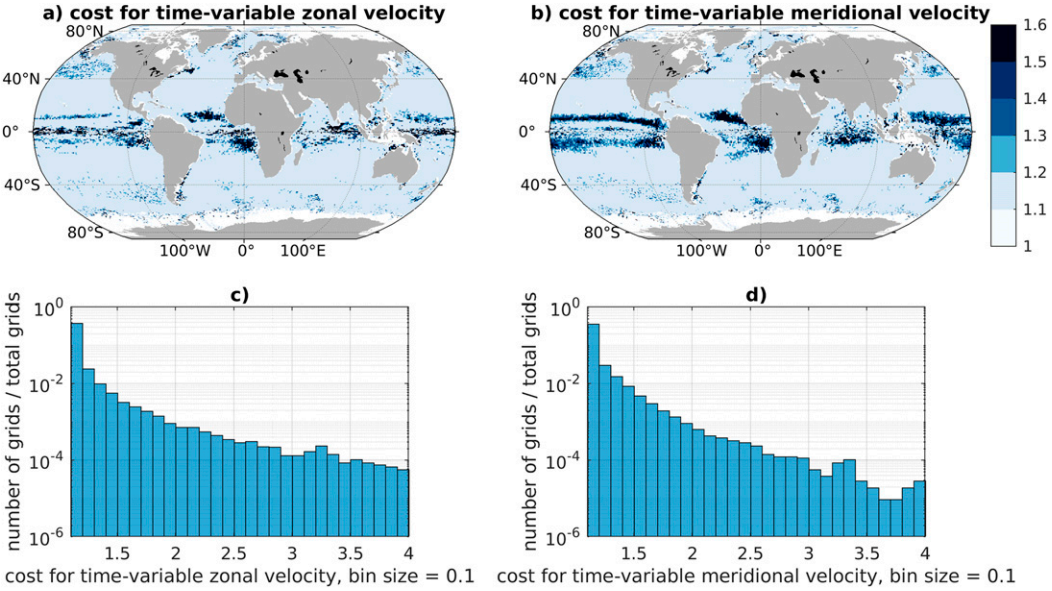

FIG. 6. (a),(b) Maps of cost for daily (a) zonal and (b) meridional velocities. (c),(d) Histograms of cost values in (a) and (b). Note that *y* axes are in log scale.

signals are larger than data errors and therefore are appropriate to be used for further analyses. However, SNR in other regions does not deviate much from one, meaning that the signal variability cannot be distinguished from ''noise.'' Substituting Eq. (1) in SNR formula, values of SNR $\sim$ 1 indicate the covariance between modeled and drifter velocities is close to zero. The low model–data covariance also explains the similar magnitude of data errors (Figs. 4a,b) computed from Eq. (1) and velocity standard deviations (Figs. 2a,c).

Errors for time-mean velocities calculated as described in section 2c show larger values in regions with major currents (Figs. 5a,c). Over these regions, errors for zonal and meridional velocities are $\sim$0.11–0.25 m s^{-1}. In the basin interior, errors are generally smaller than 0.05 m s^{-1}. These values contain both instrument and representation errors, together with biases associated with undersampling of mesoscale variability. We attempt to separate these errors by examining error estimates given by method 2 (see section 2c), which are considered to be mostly sampling related errors (Figs. 5b,d). The latter errors yield values of $\sim$0.05–0.15 m s^{-1} in energetic regions and $<$0.03 m s^{-1} in quieter areas. Given that instrument errors from calibrated drifter velocities should be small, this suggests that representation errors play a substantial role in regions of major currents as expected from some of the fine structure associated, for example, with the ACC, the Gulf Stream, and the Kuroshio.

b. Constraining ECCO velocity field

We use *cost* to evaluate the potential of constraining ECCO velocity field with GDP data, as introduced in section 2d. The cost estimates for time-variable velocities, calculated as $\langle (D-M)^2/\varepsilon_D^2 \rangle$, are presented in Fig. 6, based on errors in Fig. 4. Note that since we cap time-variable data error variances within 10% and 90% of var$(D-M)$, our estimated cost values naturally range between 1.1 and 10. Cost in $\sim$55% of the ocean grids are affected by the capping. There are very few areas in Fig. 6 with cost values substantially greater than one. Higher cost values (1.3–1.6) are found along latitudes $\sim$10°N and $\sim$10°S and in the North Pacific. Together with low SNR (Figs. 4e,f), we conclude that the influence of using GDP measurements in constraining the variability in ECCO daily surface velocity field would be limited mostly to low latitude regions, which have currents that are primarily wind driven and relatively large scale, and where representation errors are somewhat weaker. Better advantage of the GDP data would likely result from increased model resolutions, to be able to represent more of the mesoscale and smaller features captured by the drifters. Cost estimates for monthly surface velocities are similar to those for daily velocities and are not shown here.

Regarding time-mean surface currents, constraining ECCO using the GDP climatology seems more important, as shown in the maps of cost (Figs. 7a,b) calculated as the ratio of the square of the ECCO–GDP differences over the square of the errors in Figs. 5a and 5c. Cost values substantially greater than 1 can be found in many regions. Particularly for zonal velocities, extensive areas in the tropics as well as in some subtropical basin interiors show costs greater than 2. For meridional velocities, areas with cost values greater than 1 are still present but tend to be smaller and less well organized.

The somewhat spatially noisy character of the cost in Figs. 7a and 7b could be mostly owing to the short-scale structures sampled by drifters. To be more effective, one can attempt to apply constraints based on larger-scale velocity features. We explore these effects by calculating costs based on GDP–ECCO misfits spatially smoothed over 3° $\times$ 3° boxes, with corresponding errors estimated from the similarly smoothed differences between the GDP and OSCAR time-mean velocities (Figs. 7e,f). Coherent areas with costs greater than 1 that

Brought to you by NOAA Central Library | Unauthenticated | Downloaded 04/20/21 02:47 PM UTC

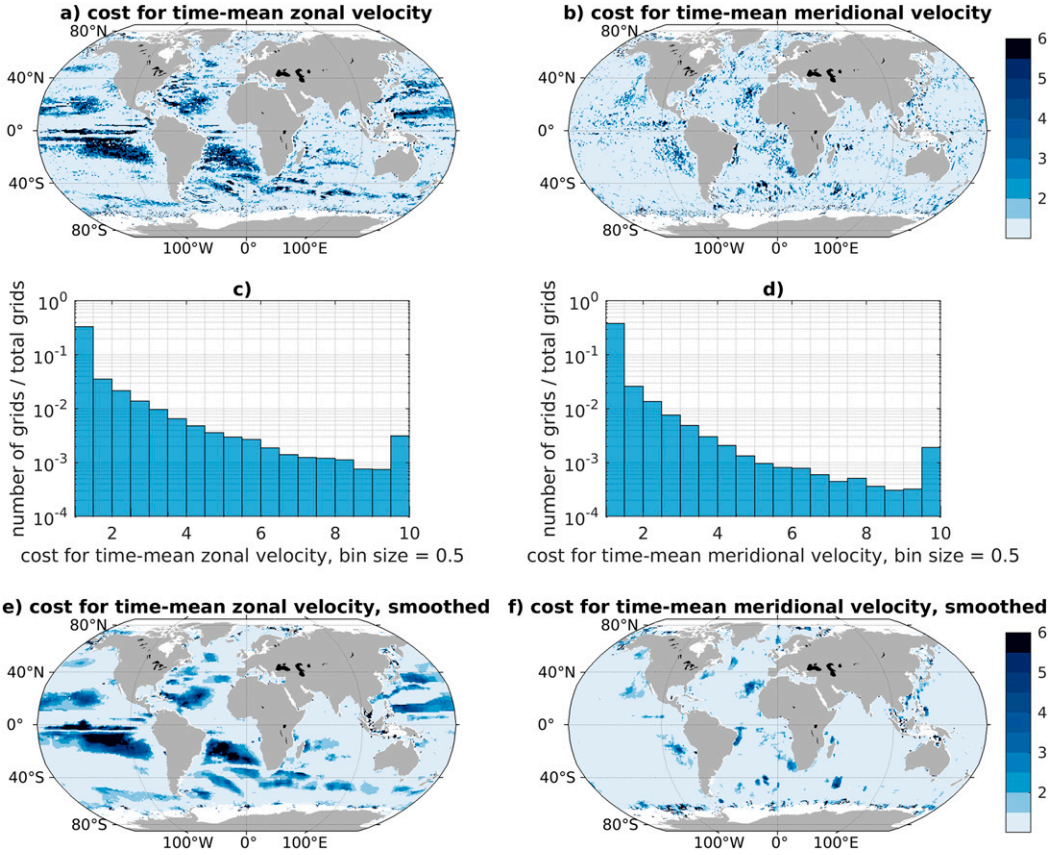

FIG. 7. (a),(b) Maps of cost for time-mean (a) zonal and (b) meridional velocities. (c),(d) Histograms of cost values in the maps in (a) and (b). Note that *y* axes are in log scale. (e),(f) Maps of cost for time-mean (e) zonal and (f) meridional velocities, with cost values calculated based on smoothed GDP–ECCO misfits and smoothed GDP–OSCAR differences.

are more spatially smooth remain visible and are clearer for meridional velocities. These results indicate that GDP constraints, either at original resolutions or in some spatially averaged form, could affect the surface current representation in ECCO state estimates.

5. Summary and discussion

In this paper, we have examined the nature of the surface currents determined from GDP data in comparison with those simulated by an ECCO model run for the period 1992–2017. A main motivation was to explore the potential for improving circulation estimates by constraining coarse-resolution climate-type models to drifter measurements. The mean and variability of GDP currents are comparable in magnitude to the model currents at low latitudes, where large-scale wind-driven currents tend to dominate, but they are considerably larger elsewhere, reflecting in part the presence of short-scale features in boundary currents and eddies that are not represented in the coarse-resolution model. Using the model–data comparisons, data errors for time-variable and time-mean velocities were estimated separately. These errors contain both instrument noise and representation errors associated with data–model mismatch in resolution or deficiencies in model physics. Model–data misfits were then evaluated based on the error estimates.

For time-variable (daily and monthly) velocities, differences between ECCO and GDP are found not to be substantially larger than data errors over most regions. Potential impacts of incorporating drifter velocity constraints in ECCO optimization procedures would be limited mostly to low latitudes. For time-mean velocities, differences between model and data can be substantially larger than the estimated data errors, indicating that modeled surface currents in a wide range of areas could be improved through constraints to drifter velocities.

In fact, the surface velocity field from the latest optimized ECCO estimate (version 4, release 4; https://ecco-group.org/products-ECCO-V4r4.htm; Fukumori et al. 2019) is found to be closer to the GDP data than that from the control run used here (not shown). Such behavior indicates that other data constraints (e.g., altimetry, geodetic MDT) used in the ECCO estimate cause the surface circulation to be closer to that implied by the GDP data. This is consistent with our inference that GDP data contain relevant information for constraining ECCO solutions. Using the error estimates derived in this work, GDP velocities are currently being incorporated into the

Brought to you by NOAA Central Library | Unauthenticated | Downloaded 04/20/21 02:47 PM UTC

ECCO inverse modeling framework together with other variables. One interesting question for future study is whether the drifters can bring extra information to the optimization problem relative to all the other datasets.

Previous use of drifter data in improving MDT estimates (e.g., Rio and Hernandez 2004) involves removing the ageostrophic component of the surface velocity to focus on the geostrophic flow related to the surface height gradients. One advantage of the proposed ECCO optimization with drifter constraints is that one makes full use of the information in the drifter measurements. Such information can help constrain the geostrophic as well as ageostrophic components of the surface circulation.

The use of all data, including drifters, in an ECCO-like optimization procedure should lead to improved estimates of the full surface circulation and likely improved MDT estimates as well. The latter fields can be used in turn to derive better estimates of the marine geoid for comparison with those derived from GRACE and other space geodesy measurements. To the extent that the surface circulation is dependent on air–sea momentum transfers and kinetic energy dissipation, assimilation of GDP data can also lead to more realistic boundary forcing and subgrid-scale physical parameterizations needed for accurate descriptions of surface circulations in climate models.

Some limitations of our results are worth noting. Errors for time-variable velocities are calculated based on the assumption of negligible mutual correlation between data error, model error, and the common velocity signal. Violation of this assumption may cause biased error estimates. Similar issues can affect the estimated time-mean errors. In addition, there are some inevitable arbitrary assumptions in bounding the errors, but such measures attempt to mitigate extreme overfitting or underfitting that can lead to problems in constrained optimization procedures. In this context, the combined use of different datasets as proposed here can help expose inconsistencies and potential issues with error estimates.

Acknowledgments. This study is funded by the GRACE Follow-On Science Team through NASA Grant 80NSSC20K0728 to AER. Support for the ECCO project is provided by the NASA Physical Oceanography, Cryospheric Science, and Modeling, Analysis and Prediction programs. Part of the research was carried out at the Jet Propulsion Laboratory, California Institute of Technology, under a contract with the National Aeronautics and Space Administration (80NM0018D0004). R. Lumpkin was supported by NOAA's Global Ocean Monitoring and Observing Program and the Atlantic Oceanographic and Meteorological Laboratory.

Data availability statement. Drifter velocity data used in this study are provided by Dr. Rick Lumpkin and available at ftp://ftp.aoml.noaa.gov/phod/pub/lumpkin/mengnan; data were accessed on 24 July 2019. Error estimates are openly available at ftp://ftp.aoml.noaa.gov/phod/pub/lumpkin/drifter_climatology. The OSCAR product can be downloaded from the NASA Physical Oceanography Data Center at https://podaac.jpl.nasa.gov/dataset/OSCAR_L4_OC_third-deg and was accessed on 28 May 2019. Velocity data at second vertical level from ECCO control run are available at https://ecco.jpl.nasa.gov/drive/files/Version4/Release4/other/control_run.

REFERENCES

Aleynik, D., A. C. Dale, M. Porter, and K. Davidson, 2016: A high resolution hydrodynamic model system suitable for novel harmful algal bloom modelling in areas of complex coastline and topography. *Harmful Algae*, **53**, 102–117, https://doi.org/10.1016/j.hal.2015.11.012.

Blockley, E., M. Martin, and P. Hyder, 2012: Validation of foam near-surface ocean current forecasts using Lagrangian drifting buoys. *Ocean Sci.*, **8**, 551–565, https://doi.org/10.5194/os-8-551-2012.

Bonjean, F., and G. S. Lagerloef, 2002: Diagnostic model and analysis of the surface currents in the tropical Pacific Ocean. *J. Phys. Oceanogr.*, **32**, 2938–2954, https://doi.org/10.1175/1520-0485(2002)032<2938:DMAAOT>2.0.CO;2.

Dee, D. P., and Coauthors, 2011: The ERA-Interim reanalysis: Configuration and performance of the data assimilation system. *Quart. J. Roy. Meteor. Soc.*, **137**, 553–597, https://doi.org/10.1002/qj.828.

de La Lama, M. S., J. LaCasce, and H. K. Fuhr, 2016: The vertical structure of ocean eddies. *Dyn. Stat. Climate Syst.*, **2016**, 2938–2954, https://doi.org/10.1093/CLIMSYS/DZW001.

Drews, A., and R. J. Greatbatch, 2016: Atlantic multidecadal variability in a model with an improved North Atlantic Current. *Geophys. Res. Lett.*, **43**, 8199–8206, https://doi.org/10.1002/2016GL069815.

Elipot, S., and S. T. Gille, 2009: Estimates of wind energy input to the Ekman layer in the Southern Ocean from surface drifter data. *J. Geophys. Res.*, **114**, C06003, https://doi.org/10.1029/2008JC005170.

ESR, 2009: OSCAR third degree resolution ocean surface currents, version 1. PO.DAAC, accessed 28 May 2019, https://doi.org/10.5067/OSCAR-03D01.

Forget, G., J.-M. Campin, P. Heimbach, C. N. Hill, R. M. Ponte, and C. Wunsch, 2015: ECCO version 4: An integrated framework for non-linear inverse modeling and global ocean state estimation. *Geosci. Model Dev.*, **8**, 3071–3104, https://doi.org/10.5194/gmd-8-3071-2015.

Fukumori, I., O. Wang, I. Fenty, G. Forget, P. Heimbach, and R. M. Ponte, 2017: ECCO version 4 release 3. California Institute of Technology Tech. Rep., 10 pp.

——, ——, ——, ——, ——, and ——, 2019: ECCO version 4 release 4. California Institute of Technology Tech. Rep. 17 pp.

Hansen, D. V., and P.-M. Poulain, 1996: Quality control and interpolations of WOCE-TOGA drifter data. *J. Atmos. Oceanic Technol.*, **13**, 900–909, https://doi.org/10.1175/1520-0426(1996)013<0900:QCAIOW>2.0.CO;2.

Hausman, J., F. Bonjean, and K. Dohan, 2009: Ocean Surface Current Analysis (OSCAR) third degree resolution user's handbook. California Institute of Technology Doc., 10 pp., https://podaac-tools.jpl.nasa.gov/drive/files/allData/oscar/preview/L4/oscar_third_deg/docs/oscarthirdguide.pdf.

Hui, Z., and Y. Xu, 2016: The impact of wave-induced Coriolis-Stokes forcing on satellite-derived ocean surface currents. *J. Geophys. Res. Oceans*, **121**, 410–426, https://doi.org/10.1002/2015JC011082.

Johnson, E. S., F. Bonjean, G. S. Lagerloef, J. T. Gunn, and G. T. Mitchum, 2007: Validation and error analysis of OSCAR sea surface currents. *J. Atmos. Oceanic Technol.*, **24**, 688–701, https://doi.org/10.1175/JTECH1971.1.

Brought to you by NOAA Central Library | Unauthenticated | Downloaded 04/20/21 02:47 PM UTC

Kawaguchi, Y., S. Nishino, and J. Inoue, 2015: Fixed-point observation of mixed layer evolution in the seasonally ice-free Chukchi Sea: Turbulent mixing due to gale winds and internal gravity waves. *J. Phys. Oceanogr.*, **45**, 836–853, https://doi.org/10.1175/JPO-D-14-0149.1.

Kelly, K. A., and S. Dong, 2004: The relationship of western boundary current heat transport and storage to midlatitude ocean-atmosphere interaction. *Earth's Climate: The Ocean–Atmosphere Interaction*, *Geophys. Monogr.*, Vol. 147, Amer. Geophys. Union, 347–363.

Knudsen, P., O. Andersen, and N. Maximenko, 2021: A new ocean mean dynamic topography model, derived from a combination of gravity, altimetry and drifter velocity data. *Adv. Space Res.*, https://doi.org/10.1016/j.asr.2019.12.001, in press.

Kubryakov, A., and S. Stanichny, 2011: Mean dynamic topography of the Black Sea, computed from altimetry, drifter measurements and hydrology data. *Ocean Sci.*, **7**, 745–753, https://doi.org/10.5194/os-7-745-2011.

Laurindo, L. C., A. J. Mariano, and R. Lumpkin, 2017: An improved near-surface velocity climatology for the global ocean from drifter observations. *Deep-Sea Res. I*, **124**, 73–92, https://doi.org/10.1016/j.dsr.2017.04.009.

Lozovatsky, I., H. Wijesekera, E. Jarosz, M.-J. Lilover, A. Pirro, Z. Silver, L. Centurioni, and H. Fernando, 2016: A snapshot of internal waves and hydrodynamic instabilities in the southern Bay of Bengal. *J. Geophys. Res. Oceans*, **121**, 5898–5915, https://doi.org/10.1002/2016JC011697.

Lumpkin, R., and P. J. Flament, 2013: Extent and energetics of the Hawaiian Lee Countercurrent. *Oceanography*, **26** (1), 58–65, https://doi.org/10.5670/oceanog.2013.05.

——, and L. Centurioni, 2019: Global drifter program quality-controlled 6-hour interpolated data from ocean surface drifting buoys. NOAA National Centers for Environmental Information, accessed 24 July 2019, https://doi.org/10.25921/7ntx-z961.

Müller, V., D. Kieke, P. G. Myers, C. Pennelly, R. Steinfeldt, and I. Stendardo, 2019: Heat and freshwater transport by mesoscale eddies in the southern subpolar North Atlantic. *J. Geophys. Res. Oceans*, **124**, 5565–5585, https://doi.org/10.1029/2018JC014697.

Niiler, P. P., A. S. Sybrandy, K. Bi, P. M. Poulain, and D. Bitterman, 1995: Measurements of the water-following capability of Holey-Sock and Tristar drifters. *Deep-Sea Res. I*, **42**, 1951–1964, https://doi.org/10.1016/0967-0637(95)00076-3.

Petersen, M. R., and Coauthors, 2019: An evaluation of the ocean and sea ice climate of E3SM using MPAS and interannual CORE-II forcing. *J. Adv. Model. Earth Syst.*, **11**, 1438–1458, https://doi.org/10.1029/2018MS001373.

Poulain, P.-M., R. Gerin, E. Mauri, and R. Pennel, 2009: Wind effects on drogued and undrogued drifters in the eastern Mediterranean. *J. Atmos. Oceanic Technol.*, **26**, 1144–1156, https://doi.org/10.1175/2008JTECHO618.1.

Pringle, J. M., J. E. Byers, P. Pappalardo, J. P. Wares, and D. Marshall, 2014: Circulation constrains the evolution of larval development modes and life histories in the coastal ocean. *Ecology*, **95**, 1022–1032, https://doi.org/10.1890/13-0970.1.

Qian, Y.-K., S. Peng, C.-X. Liang, and R. Lumpkin, 2014: On the estimation of Lagrangian diffusivity: Influence of nonstationary mean flow. *J. Phys. Oceanogr.*, **44**, 2796–2811, https://doi.org/10.1175/JPO-D-14-0058.1.

Quinn, K. J., and R. M. Ponte, 2008: Estimating weights for the use of time-dependent gravity recovery and climate experiment data in constraining ocean models. *J. Geophys. Res.*, **113**, C12013, https://doi.org/10.1029/2008JC004903.

Rio, M.-H., and F. Hernandez, 2004: A mean dynamic topography computed over the world ocean from altimetry, in situ measurements, and a geoid model. *J. Geophys. Res.*, **109**, C12032, https://doi.org/10.1029/2003JC002226.

——, S. Mulet, and N. Picot, 2014: Beyond GOCE for the ocean circulation estimate: Synergetic use of altimetry, gravimetry, and in situ data provides new insight into geostrophic and Ekman currents. *Geophys. Res. Lett.*, **41**, 8918–8925, https://doi.org/10.1002/2014GL061773.

Sallée, J.-B., R. Morrow, and K. Speer, 2008: Eddy heat diffusion and subantarctic mode water formation. *Geophys. Res. Lett.*, **35**, L05607, https://doi.org/10.1029/2007GL032827.

Sikhakolli, R., R. Sharma, S. Basu, B. Gohil, A. Sarkar, and K. Prasad, 2013: Evaluation of OSCAR ocean surface current product in the tropical Indian Ocean using in situ data. *J. Earth Syst. Sci.*, **122**, 187–199, https://doi.org/10.1007/s12040-012-0258-7.

Small, R. J., and Coauthors, 2008: Air–sea interaction over ocean fronts and eddies. *Dyn. Atmos. Oceans*, **45**, 274–319, https://doi.org/10.1016/j.dynatmoce.2008.01.001.

Sudre, J., C. Maes, and V. Garçon, 2013: On the global estimates of geostrophic and Ekman surface currents. *Limnol. Oceanogr. Fluids Environ.*, **3** (1), 1–20, https://doi.org/10.1215/21573689-2071927.

Sun, L., and S. G. Penny, 2019: Lagrangian data assimilation of surface drifters in a double-gyre ocean model using the local ensemble transform Kalman filter. *Mon. Wea. Rev.*, **147**, 4533–4551, https://doi.org/10.1175/MWR-D-18-0406.1.

Vinogradova, N. T., R. M. Ponte, I. Fukumori, and O. Wang, 2014: Estimating satellite salinity errors for assimilation of Aquarius and SMOS data into climate models. *J. Geophys. Res. Oceans*, **119**, 4732–4744, https://doi.org/10.1002/2014JC009906.

Wang, O., I. Fukumori, and I. Fenty, 2019: ECCO version 4 release 4 user guide. JPL Doc., 14 pp., https://ecco-group.org/docs/v4r4_user_guide.pdf.

Wunsch, C., 1997: The vertical partition of oceanic horizontal kinetic energy. *J. Phys. Oceanogr.*, **27**, 1770–1794, https://doi.org/10.1175/1520-0485(1997)027<1770:TVPOOH>2.0.CO;2.

——, P. Heimbach, R. M. Ponte, and I. Fukumori, 2009: The global general circulation of the ocean estimated by the ECCO-Consortium. *Oceanography*, **22** (2), 88–103, https://doi.org/10.5670/oceanog.2009.41.

Yu, X., A. L. Ponte, S. Elipot, D. Menemenlis, E. D. Zaron, and R. Abernathey, 2019: Surface kinetic energy distributions in the global oceans from a high-resolution numerical model and surface drifter observations. *Geophys. Res. Lett.*, **46**, 9757–9766, https://doi.org/10.1029/2019GL083074.

Zhurbas, V., and I. S. Oh, 2003: Lateral diffusivity and Lagrangian scales in the Pacific Ocean as derived from drifter data. *J. Geophys. Res.*, **108**, 3141, https://doi.org/10.1029/2002JC001596.

Brought to you by NOAA Central Library | Unauthenticated | Downloaded 04/20/21 02:47 PM UTC